Materials and Design 31 (2010) 2670–2675

Contents lists available at ScienceDirect

Materials and Design

journal homepage: www.elsevier.com/locate/matdes

Short Communication

Hardness and wear resistance improvement of surface composite layer on Ti–6Al–4V substrate fabricated by powder sintering

Rui-Hua Hu, Jae-Kyoo Lim *

Automobile High Technology Research Institute, Department of Mechanical Design, Chonbuk National University, Deokjin 1-664-14, Jeonju, Republic of Korea

ARTICLE INFO

Article history:
Received 11 August 2009
Accepted 26 November 2009
Available online 3 December 2009

ABSTRACT

A wear resistant surface composite layer on Ti–6Al–4V substrate was fabricated using powder sintering method. The surface composite layer consisted of Ti–6Al–4V matrix and different fractions of TiN particles as reinforcement phase. The surface layer and the substrate were directly bonded together while the powders were cold formed and then sintered at an elevated temperature. The two layers showed good metallurgical bond. In this study, 5%, 10% and 15% TiN weight fractions were adopted to fabricate the surface composite layer. Effects of TiN addition on the microstructure, hardness and wear resistance were investigated. It was found that the wear resistance of the surface composite layer was improved due to the addition of TiN compared to that of pure Ti–6Al–4V.

1. Introduction

Titanium and its alloys, due to their excellent properties such as high strength-to-weight ratio, good mechanical properties at elevated temperatures, corrosion resistance and biocompatibility, have been used for chemical, electric power, aerospace, automobile and medical applications. However, the main drawbacks of titanium and its alloys are their low hardness and poor resistance to sliding wear.

In order to improve the tribological property of titanium and its alloys, many methods such as surface coating [1–3], surface nitriding [4,5], and surface cladding [6–8] have been developed. Although surface coating and surface nitriding layer are very thin films with thickness from several micrometers to hundreds micrometers, the coated samples show much improvement of wear resistance. Likewise, surface cladding shows better wear durability in circumstances of friction under high contact stress on soft substrate like Ti and its alloys.

To achieve higher wear durability, bimetal structure can offer advantages by increasing the hardness and thickness of wear resistant layer. A traditional way of making such structures is to weld or bond hard layer together with another metal. In addition to the high cost associated with the secondary operations, the conventional joining approach also has the disadvantage of requiring the use of a third material (e.g., weld fillers, adhesives, etc.). In recent years, powder metallurgy methods have been employed to fabricate bimetal with ceramic powders like SiC, TiB_2 and TiC using laser or electron beam radiation [9–13]. The thickness of the cladding layer fabricated by such methods can be up to several millimeters.

Up to now, the investigation of a comparatively feasible method—powder sintering to make wear resistant surface layer has been seldom reported. Powder sintering is a near-net-shape forming method. It provides the possibility to form composites containing various additives that may improve some properties of the composites. Meanwhile, it possesses the flexibility to obtain dimension as needed. To fabricate a wear resistant layer with required thickness and enhanced hardness, powder sintering method is adopted in this research. The objective of this research is to fabricate a surface composite layer with TiN addition. Its microstructure and the improvement of hardness and wear resistance are also investigated.

2. Materials and methods

Ti–6Al–4V powder with average particle size 56 μm was supplied by Se-Jong Materials Ltd., Korea. The chemical compositions of the Ti–6Al–4V powder are shown in Table 1. The TiN powder contains 99.5% TiN, purchased from Sigma–Aldrich Inc. The main impurities of TiN powder are listed below: Al < 6 ppm, Cr < 5 ppm, Mn < 5 ppm, Pb < 35 ppm.

The detailed sample preparation process is indicated in Fig. 1. Pure Ti–6Al–4V powders and mixed powders containing different fractions of TiN (5%, 10%, and 15% (wt.), respectively) were firstly prepared. The mixed powders were blended on a ball milling machine for 24 h. Then the pure powders and mixed powders were successively poured into the mould. Subsequently, the powders were pressed in a mould with 380 MPa pressure using an uniaxial press machine to make green body. All samples were then vacuum

* Corresponding author. Tel.: +82 63 270 2321; fax: +82 63 270 4439.
E-mail address: jklim@chonbuk.ac.kr (J.-K. Lim).

0261-3069/$ - see front matter © 2009 Elsevier Ltd. All rights reserved.
doi:10.1016/j.matdes.2009.11.057

Table 1
Chemical composition of Ti–6Al–4V powders (wt.%).

Element	Al	V	O	N	H	Zr	Fe	Ti
wt.%	6.62	4.55	0.55	0.5	0.3	0.03	0.02	Bal.

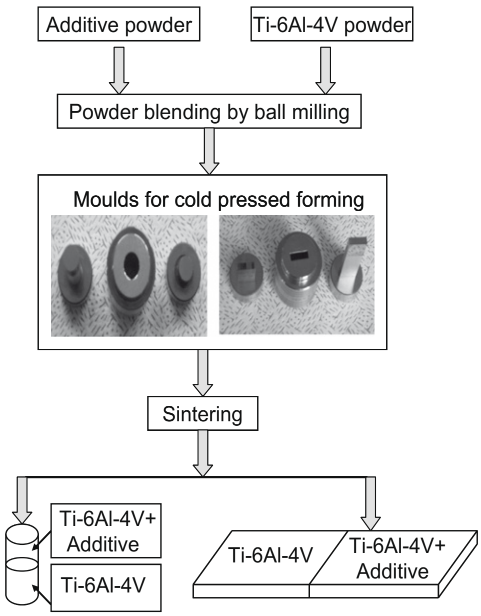

Fig. 1. Sample preparation process.

sintered (the absolute pressure was 20 millitorr). The temperature was increased from room temperature to 1250 °C within 3 h and held at 1250 °C for 4 h, and then cooled down to room temperature within 2 h. Our previous research [11] proved that pure Ti–6Al–4V by sintering has good microstructure, compressive strength (600 MPa) and hardness (HRC 28.4). Therefore, the above sintering procedure was still adopted in this research. Also it was reported that the mechanical properties of the samples sintered at 1200 °C for 3–6 h can be up to the JIS 60 grade of wrought Ti–6Al–4V and above 95% relative density [14,15].

Cylindrical and rectangular samples were fabricated by using two kinds of mould. Different thickness of the surface layer can be obtained by metering the amount of mixed powders.

Specimens with different TiN fractions for microstructure observation were polished by sand paper and alumina slurries, and etched with Kroll's etchant (5% nitric acid, 10% HF, and 85% water). The Vickers hardness of the matrix was measured by a digital hardness tester (Model: MXT CX7) with a 200 g load according to ASTM E384-99. At least 10 successive measurements were carried out for each sample. The Rockwell hardness was also tested. The microstructures of the specimens were observed by optical microscopy and scanning electron microscope (SEM). X-ray diffraction (XRD) was also employed to identify the phases of the sintered materials.

Wear test was conducted using a pin-on-disk wear testing machine. The sample was in the form of a cylindrical pin with 11 mm in diameter, and 10 mm in length. The contact surfaces of these pins were polished to 0.3 μm roughness and rubbed against a hardened stainless steel disk with the roughness of 0.3 μm and hardness of 62 HRC. All wear tests were carried out at an applied normal load of 150 N, and a linear velocity of 15 m/min. The total sliding distance was 1500 m. The test was conducted at room temperature without lubricant. The wear resistance was measured in terms of weight loss of the tested samples using a precision balance. In the same wear testing condition, wear weight loss of the pure Ti–6Al–4V and Ti–6Al–4V with TiN additions were tested and compared. After testing, wear scars on the wear surface and wear debris were observed by using microscope.

3. Results and discussion

3.1. Morphology of interface, microstructure analysis and phase identification

The samples consisting of Ti–6Al–4V substrate and surface composite layer were successfully fabricated. As shown in Fig. 2a, the two layers can be identified by their minor difference of color, and the interface between the two layers is shown as a small step due to the different contraction of the two layers. The view from the surface of the sintered sample is shown in Fig. 2b. A magnified morphology of the interface between the two layers can be seen clearly, which are shown in Fig. 2b and c. No cracks and delaminating were found near to the interface. The surface layer and the substrate showed different shrinkage during sintering, which can be observed by the changes of their sizes. The surface layer showed a larger shrinkage than the substrate. Fig. 2d shows a polished and etched surface of a cross section near to the interface. In microscopic scale, a clear boundary between the two layers cannot be found (Fig. 2d), however, the differences of grain size and morphology in the interface field can be identified. In the substrate, the grains show plate-like and acicular, and the grain boundaries are thicker. In contrast, the grains show mostly larger plate-like in the surface layer, and the grain boundaries are thin. Some small particles embedded in the matrix can be observed in the surface layer. In microscopic scale, the two layers show good metallurgical bond. Neither micro cracks nor delamination was found around the interface.

A slice was cut from the end of the composite layer of a cylindrical specimen to make a sample for XRD analysis. The remaining part was polished for optical microstructure observation. Fig. 3 shows XRD patterns of sintered Ti–6Al–4V (Fig. 3a) and Ti–6Al–4V with 10% TiN addition (Fig. 3b). The patterns indicate that Ti–6Al–4V consists of alpha and beta phases, and that Ti–6Al–4V with TiN addition consists of only alpha phase and TiN.

Fig. 4 indicates the metallographic photos of the sintered materials. The microstructure of pure Ti–6Al–4V consists of plate-like and acicular alpha (light) phase and intergranular beta phase (dark), as presented in Fig. 4a. This shows a typical slowly cooling-down equilibrium microstructure.

As shown in Fig. 4b, the microstructure of Ti–6Al–4V with 5% TiN addition consists of mostly plate-like and little acicular alpha phase. Intergranular beta phase was not observed. Meanwhile, a few of uniformly dispersed TiN particles can be found in the matrix. With the amount increasing of TiN addition, the microstructures consist of pure plate-like alpha phase and more TiN particles, which are indicated in Fig. 4c and d.

The fact that beta phase disappears in the microstructure of Ti–6Al–4V samples is due to TiN addition. This can be attributed to nitrogen solution from part of TiN to the matrix, because nitrogen is a promoter of alpha phase formation, which can be seen from the TiN phase diagram [16]. Nitrogen dissolution enhances the transformation temperature from hcp to bcc. Moreover, nitrogen dissolved from TiN forms the N-rich matrix and causes solid-solution hardening of the matrix. Fig. 4b–d shows that the number of TiN particles gradually increases, and they are more densely dispersed in the matrix with the amount increasing of TiN addition. Metallic matrix containing reinforcement particles is known as metallic matrix composite (MMC). Kim [17] investigated the effects of particles on the hardness of particulate reinforced

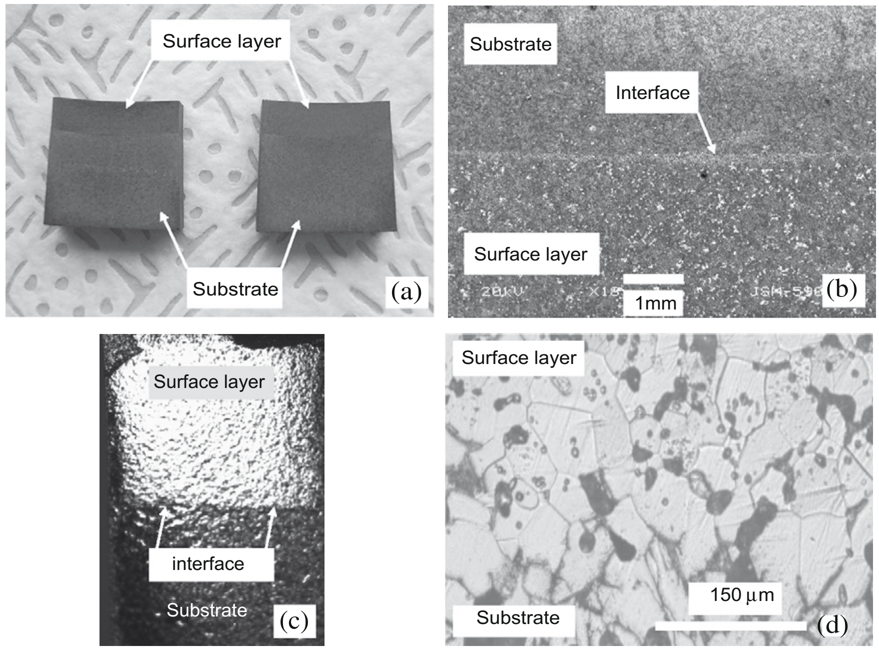

Fig. 2. (a) Morphology of the sintered samples, (b) view of interface from as-sintered sample surface, (c) polished cross section of the sample, (d) microscopic photo near to the interface.

composites. Under certain circumstances, the hardness can be improved by particle addition. Therefore, according to above observation, an improvement of hardness of the sintered material can be expected.

3.2. Hardness testing results

Hardness is regarded as an indicative of wear resistance. Therefore micro Vickers hardness and bulk hardness were tested. Micro Vickers hardness was tested selectively on the matrix. It was noted that the Vickers hardness scattered in a wider range. The results of the average value and standard deviation are shown in Fig. 5. With the increase of the amount of TiN addition, Vickers hardness increases very significantly. The average micro Vickers hardness of pure Ti–6Al–4V sintered in the same condition is 390. The Vickers hardness of the composites with different amount of TiN addition are 479 ± 30.5, 519 ± 52.9, 625 ± 42.6, gaining 22%, 33%, and 60% increment respectively (for 5%, 10%, and 15% TiN addition) compared to pure Ti–6Al–4V. The micro Vickers hardness enhancement of the matrix is caused by the formation of TiN solid-solution owing to the partial solution of nitrogen from TiN.

Similarly, as shown in Fig. 6, the overall bulk hardness which was tested as HRC (Rockwell hardness) has a significant increment. The overall hardness increases with the amount of TiN addition. The overall hardness value of the composite with different amount of TiN additions (5%, 10%, and 15%) are 38.48%, 41.1%, and 43.4%, gaining 35.5%, 44.6% and 52.8% increment respectively, compared to the overall hardness of pure Ti–6Al–4V (average HRC = 28.4 ± 0.84).

Bulk hardness enhancement can be attributed to the combined effect of the matrix hardening and the TiN particles embedded into the hardened matrix. In Fig. 6, the relation of hardness and the amount of TiN addition showed the tendency that the increment of hardness is related to the fraction of TiN addition, which are consistent to the prediction results according to the rule of mixture of composite materials [17].

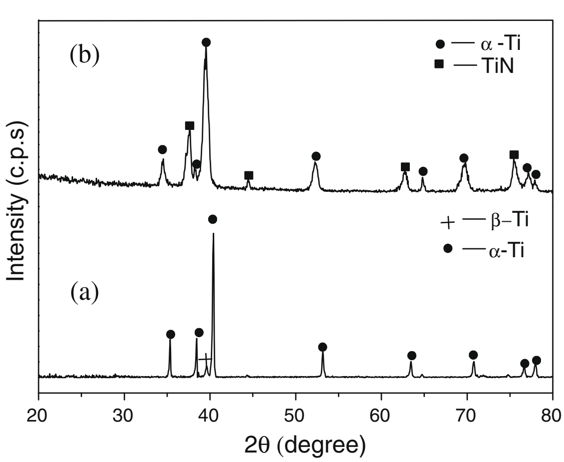

Fig. 3. XRD patterns: (a) pure Ti–6Al–4V and (b) Ti–6Al–4V with 10% TiN addition.

3.3. Wear resistance testing results

Fig. 7 demonstrates the wear weight loss after a 1500 m sliding distance on a stainless steel disk with a normal load of 150 N on the samples. It is seen clearly that the wear weight loss of all surface composite layer are lower than that of pure Ti–6Al–4V (in the same condition, wear weight loss of pure Ti–6Al–4V is 0.143 g), that is to say, the wear resistance of Ti–6Al–4V is improved by forming a composite layer on its surface.

The wear volume of Ti–6Al–4V and surface composite layer can be expressed by Archard equation [18]

$$V = \frac{kWS}{3H} \tag{1}$$

where V is the sliding wear volume; W is the normal load; S is the total sliding distance; H is the hardness of the wearing surface; and k is a probability factor that a given contact area will fracture. According to Eq. (1), in a given wear test condition (a normal load W and a sliding distance S are given) if the hardness of the compos-

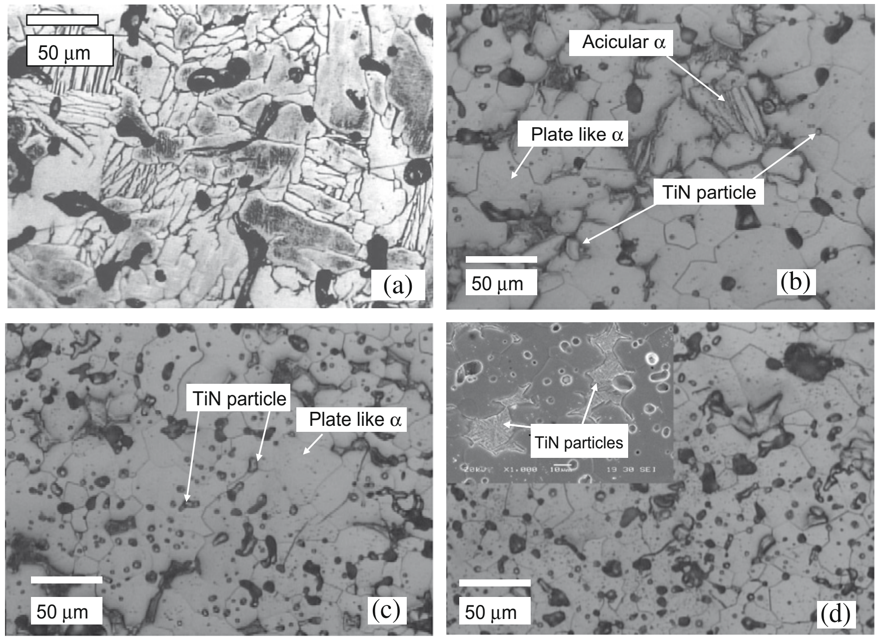

Fig. 4. Microstructure of Ti–6Al–4V and its composites: (a) pure Ti–6Al–4V, (b) 5% TiN addition, (c) 10% TiN addition, (d) 15% TiN addition.

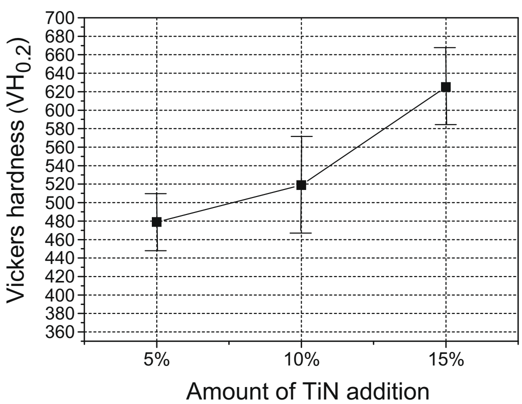

Fig. 5. Micro Vickers hardness of matrix gains as a function of TiN addition.

ite layer is enhanced, the wear volume (wear weight loss is linearly proportional to wear volume) will decrease.

After wear test, the wear surface and debris of the materials were observed by using scanning electron microscope and optical microscope. The wear scars of the pure Ti–6Al–4V and Ti–6Al–4V with 10% TiN addition are shown in Fig. 8a and b. Continuous sliding marks with deeper grooves and ridges on the surface of pure Ti–6Al–4V can be clearly observed, whereas the surface of the Ti–6Al–4V with 10% TiN addition is smooth. The smooth worn surface of the sample decreased the coefficient of friction, thus the wear was correspondingly moderated. The wear debris of the two materials are indicated in Fig. 8c and d. Larger shiny metallic flakes can be found in the wear debris of pure Ti–6Al–4V. In contrast, the debris of Ti–6Al–4V with 10% TiN addition contains only few very fine metallic flakes and mainly dark grayish particles. Wear debris may act as a very useful diagnostic tool for finding out the mechanism of wear. Larger flake-like metallic wear parti-

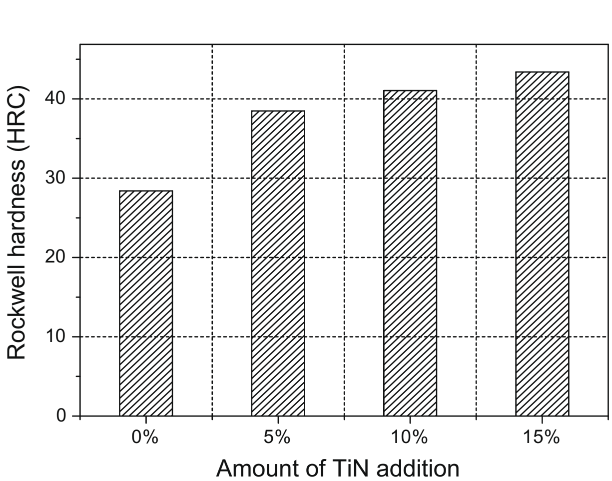

Fig. 6. Overall bulk hardness (HRC) gains as a function of TiN addition.

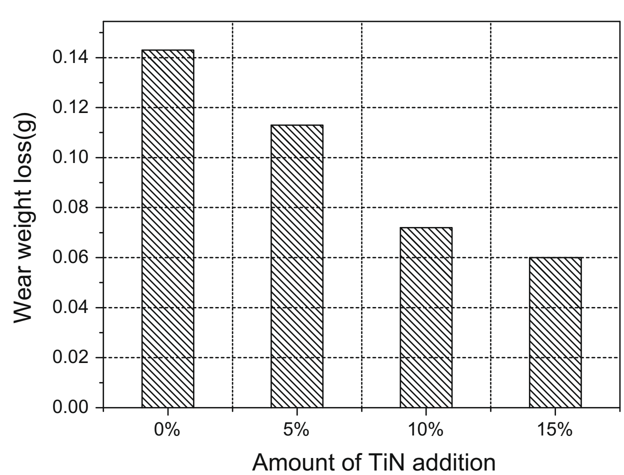

Fig. 7. Pin-on-disc sliding wear weight loss (sliding distance = 1500 m, normal load = 150 N, velocity = 15 m/min).

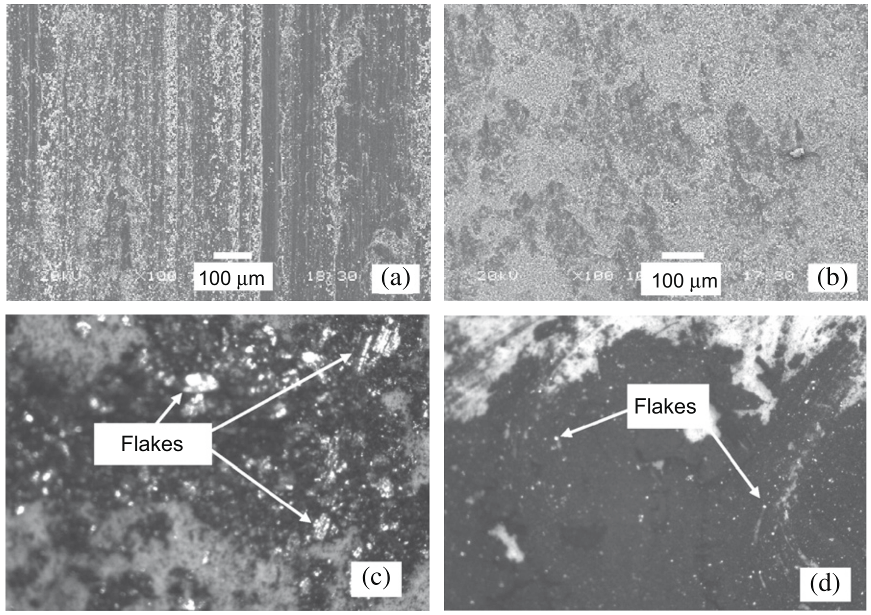

Fig. 8. Wear scars and debris: (a) wear scar on pure Ti–6Al–4V, (b) wear surface of Ti–6Al–4V with 10% TiN addition, (c) wear debris of Ti–6Al–4V, (d) wear debris of Ti–6Al–4V with 10% TiN addition.

cles indicate that delaminating occurred during wear. The grooves and ridges demonstrate that severe plastic deformation occurred. It was found that the number and size of flaky metallic wear particles in the debris decreased with the amount increasing of TiN, suggesting that plastic deformation and delaminating were largely moderated during wear due to the hardness enhancement. In addition, the surface of the wear scar of Ti–6Al–4V with 10% addition was covered by a dark film. Also, a transfer film was found on the stainless steel counter-body. The film formation was the result of oxidation because of high flash temperature while the wear test was conducted. Indeed, a test by energy dispersive spectrum(EDS) to the dark film (indicated as gray area in Fig. 9a) verifies that the film contains oxygen, as indicated in Fig. 9b. The detailed contents of the elements in the film are listed below: (O = 23.8, Al = 3.09, Ti = 65.38, V = 2.86, Fe = 4.35 and Cr = 0.52 wt.%). This film can also protect the surface and moderate the wear. The differences in worn surface characteristics among the samples can be attributed to the differences in hardness. In addition, the wear particles have an influence on the wear mechanisms. Coarse particles may cause more serious surface damage and wear weight loss by their cutting effect.

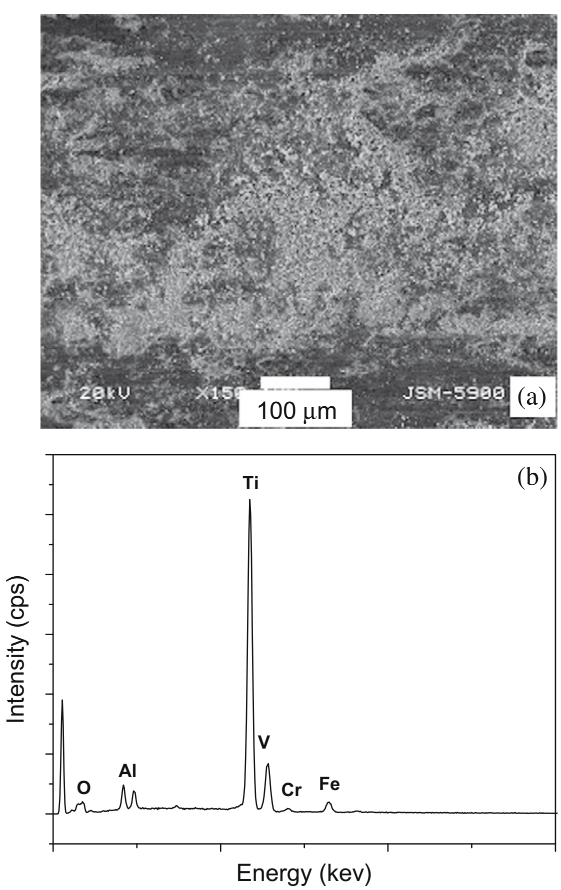

Fig. 9. EDS test result of the dark film: (a) film morphology and (b) EDS test result.

4. Conclusion

A wear resistant surface composite layer on Ti–6Al–4V substrate is fabricated by using powder sintering. Wear resistant surface layer with large thickness and higher hardness can be obtained by controlling the amount of powders and the amount of TiN addition. The surface layer and the substrate show good metallurgical bond.

The surface layer consists of Ti–6Al–4V matrix and dispersed TiN particles. The results of Vickers hardness of the matrix show a very significant increase with the addition of TiN. The combined effects of nitrogen solution and TiN particle reinforcement results in the bulk hardness increase. In addition, the hardness enhancement causes a transition of wear mechanism from dominant plastic deformation and delaminating to partial oxidation. Compared to pure Ti–6Al–4V, the sliding wear test results show that the surface layer has significant wear weight loss decrease.

Acknowledgements

This work was supported by the grant of Post-doc Program 2009, Chonbuk National University. The authors sincerely acknowledge CBNU for the support. This work was also supported by the research-oriented professor of Chonbuk National University 2009.

References

[1] Baazi T, Knystautas EJ, Fiset M. Tribomechanical properties of ion-implantation-synthesized BN films and their dependence on Ti–6Al–4V substrate hardness. Surf Coat Technol 1995;72:120–7.
[2] Vandenbulcke L, Rats D, Herbin R. Diamond coating of titanium alloys at tempering temperature. Mater Lett 1996;27:77–88.
[3] Liu Y, Erdemir A, Meletis EI. A study of the wear mechanism of diamond-like carbon films. Surf Coat Technol 1996;82:48–56.
[4] Fu YQ, Wei J, Yan BB. Characterization and tribological evaluation of duplex treatment by depositing carbon nitride films on plasma nitrided Ti–6Al–4V. J Mater Sci 2000;35:2215.
[5] Badini C, Gianoglio C, Bacci T. Characterization of surface layers in ion-nitrided titanium and titanium alloys. J Less Common Met 1988;143:129–41.
[6] Tian YS, Zhang QY, Wang DY. Study on the microstructures and properties of the boride layers laser fabricated on Ti–6Al–4V alloy. J Mater Process Technol 2009;209:2887–91.
[7] Yamamoto T, Otsuki A, Ishihara K. Synthesis of near net shape high density TiB/Ti composite. Mater Sci Eng A 1997;240:647–51.
[8] Akgun OV, Inalo T. Laser surface modification of Ti–6AI–4V alloy. J Mater Sci 1994;29:1159–68.
[9] Selamat MS, Watson LM, Baker TN. XRD and XPS studies on surface MMC layer of SiC reinforced Ti–6Al–4V alloy. J Mater Process Technol 2003;142:725–37.
[10] Yun E, Lee K, Lee S. Correlation of microstructure with high-temperature hardness of (TiC, TiN)/Ti–6Al–4V surface composites fabricated by high-energy electron-beam irradiation. Surf Coat Technol 2005;191:83–9.
[11] Yao ZP, Jiang ZH, Sun XT. Influence of the frequency on the structure and corrosion resistance of ceramic coatings on Ti–6Al–4V alloy produced by micro-plasma oxidation. Mater Chem Phys 2005;92:408–12.
[12] Hu RH, Dewidar MM, Lim JK. Effect of Si_3N_4 addition on the mechanical properties, microstructures, and wear resistance of Ti–6Al–4V alloy. J Mater Sci Technol 2007;23:257–61.
[13] Suh NP. The delamination theory of wear. Wear 1973;25:111–24.
[14] Ito Y, Hariko T, Sato K. Development of sintered Ti–6Ti–4V alloy by metal injection molding process with blended metal powders. Reports of the Hamamatsu Industrial Research Institute of Shizuoka prefecture 2003;13:7–12.
[15] Guo S, Qu X, Duan B. Influence of sintering time on mechanical properties of Ti–6Al–4V compacts by metal injection molding. Rare Met Mater Eng 2005;34:1123–8.
[16] Barrallier L, Roux L, Torregrosa F. Phase analysis, microhardness and tribological behaviour of Ti–6A1–4V after ion implantation of nitrogen in connection with its application for hip-joint prosthesis. Thin Solid Films 1995;266:245–53.
[17] Kim HS. On the rule of mixtures for the hardness of particle reinforced composites. Mater Sci Eng A 2000;289:30–3.
[18] Blau PJ. Glossary of terms, friction lubrication and wear technology in ASM handbook, vol. 18. ASM International; 1992.